Jewel Journal of Scientific Research (JJSR) 10(1): 102–111, 2025
©Federal University of Kashere-Nigeria (Print ISSN: 2384 – 6267, Online ISSN 2756-651X)
https://journals.fukashere.edu.ng/index.php/jjsr

Locating Karstic Void using Resistivity and Gravity Methods in Gua Musang, Kelantan, Malaysia

Abir, I. A.[1*], Rauff, K.O.[2], Iszar, N. I. B.[1] and Rabiu, J. A.[2]
[1]Universiti Sains Malaysia, Penang Island, 11800, Malaysia
[2]Department of Physics, Faculty of Science, Federal University of Kashere, P.M.B. 0182, Gombe, Nigeria
[2]ORCID: https://orcid.org/0000-0003-3085-5598,
***Corresponding Author**: iahmadabir@usm.my, +60125271050

Abstract
Gravity and resistivity are geophysical methods used to delineate the subsurface of the Earth. The interpretation of subsurface layers can be useful for exploration purposes and detecting anomalies that could lead to hazardous events. In this study, a CG-5 Autograv Scintrex was used to measure and collect gravity data where gravity points were calculated at 5 to 10 meters between each station. This method is conducted in a looping manner whereby, after every three (3) hour interval, the gravity points are tied to the base for the closing of the loop. These data points were then transferred into a computer for further processing and interpretation. Similarly, the resistivity method investigates variations of electrical resistance by causing electrical current to flow through the subsurface using wires connected to the ground. In this research, a dipole-dipole protocol was implemented to a 200-meter-long survey line with each line representing 100 meters from the center. The electrodes were planted every 5 meters across 6 survey lines using ABEM Terrameter SAS 4000. The obtained resistivity data were also transferred into the computer for further processing using the RES2DINV programme to create a resistivity pseudosection model. The model was further interpreted to locate the karstic void from the difference in resistivity value at different depths. The combined results from both gravity and resistivity methods gave a more accurate representation of the Earth's subsurface layers which in turn enable the location of the void to be pinpointed more accurately.

Keywords: Gravity, Resistivity, Dipole-dipole protocol, Electrodes, Pseudosection.
Received: 20th March, 2025 *Accepted:* 27th June, 2025 *Published Online:* 30th June, 2025

Introduction

When water and other substances work on carbonate rocks like limestone or dolomite, the result is a unique topography known as karst (Gambetta et al., 2011; McGrath et al., 2002; Styles et al., 2005; Thode et al., 1965). These processes form irregular structures over thousands to millions of years, including cliffs, sinkholes, caverns, subsidence, and floaters (Amaral *et al*., 2013). Finding karstic structures beneath the surface is one of the practical and significant geophysical survey research (Ahmad *et al*., 2006; Elhaj, 2016; Iqbal and Khan, 2014; Zhou *et al*., 2002). Geophysics requires understanding the Earth's subsurface to explore what is under the surface. This facilitates the investigation and detection of anomalies that may lead to hazardous circumstances. The largest district in Kelantan is Gua Musang situated in the southern part of the Malaysian province. The region is undergoing significant infrastructure and development due to its large physical area and expanding

population, yet there are some detrimental effects because of a lack of knowledge and understanding of the geological structure of the surrounding environment. The area is surrounded mostly by caves and other geological structures which are mostly covered by rocks (limestones and dolomite) (Amaral *et al*., 2013). These rocks can lead to the formation of karstic topography under the influence of water and other agents due to their physical and chemical structure that allows them to dissolve and erode easily.

The formation of karst can lead to the deformation of the subsurface layer and also lead to the occurrence of voids and cavities in the subsurface (Amaral *et al*., 2013; Chalikakis *et al*., 2011). It is therefore important to understand the geology of the area including the subsurface to avoid any structural collapses due to the instability of the bedrock. This research aims to map and analyse any possible karstic void in the study area using geophysical (Gravity and Resistivity) methods. These methods provide an accurate interpretation of the subsurface (Gochenour *et al*., 2018; Gochenour *et al*., 2017). The gravity method is used in determining the type of subsurface and locating the cavity areas while the resistivity method is used in mapping the cavities, groundwater, and depth of the bedrock.

Geology and Area of Study

Gua Musang is a district which is situated in southern Kelantan, Malaysia. The location of the field study was focused on the oil palm plantation area with the geographical coordinates of 4.87427ºN and 101.96868°E. Two formations exist in Gua Musang: Gua Musang Formation and Gunung Rabong Formation. The Gua Musang formation has existed from the Middle Permian to the Late Triassic. This formation consists of argillaceous and calcareous rock, interbedded with volcanic facies with some minor presence of arenaceous rocks. Its depositional setting exists from a shallow marine shelf deposit with active volcanic activity (Lee, 2004). Meanwhile, Gunung Rabong Formation's constituents are mainly sandstone with a minor presence of shale, mudstone, siltstone, conglomerate, and volcanic rock. Its existence is known to be formed from the Middle Triassic to the Late Triassic (Bakhshipour *et al*., 2013; Khoo, 1983).

Materials and Methods

To investigate the location of the karstic voids in Gua Musang, Kelantan, the data were acquired using two suitable geophysical (resistivity and gravity) methods. In the resistivity method, the data was acquired using a dipole-dipole array with separation of about 10 m in 200 m survey lines, and the main equipment used was ABEM Terrameter SAS 4000 with a few tools and instruments shown in Figure 1 and Table 1

Figure 1: The 2-D Electrical Resistivity Tomography (ERT) Equipment

Table 1: List of tools used and their corresponding units.

No	Tools and Instruments	Units
1.	ABEM Terrameter SAS 4000	1
2	ABEM electrode selector ES 10-64C	1
3	Battery 12V	1
4	Power Cable (12V battery to SAS 4000)	1
5	ABEM Lund Multi-Electrode Cable Connector 100m	2
6	Connection Cable (jumper)	42
7	Stainless Steel electrode	41
8	GPS	1
9	Hammer	2
10	Measuring Tape 50m	1
11	Beach Umbrella	1

Whereas, in the gravity method, data were obtained randomly using a spacing of roughly 10 m in the same survey region as the resistivity approach. The primary tool for the gravity survey is the tripod-height-adjustable CG-5 Autograv Scintrex Gravimeter. The Global Positioning System (GPS) was used to ascertain the coordinates of the base station. To show whether any spots had been moved from their initial location, the spray was utilized. Important information about the survey region and all of the data shown on the gravimeter were recorded on data sheets. Figure 2 displays the CG-5 Autograv Scintrex Gravimeter used in the gravity survey method, and Table 2 lists other tools used.

Figure 2: Equipment of the gravity measurements acquisition Scintrex CG-5 Autograv.

Table 2: Equipment List for gravity measurements acquisition Scintrex CG-5 Autograv

SN	**Equipment**
1	CG-Autograv Scintrex Gravimeter
2	Adjustable Tripod Height
3	Spray Can
4	GPS
5	Data Sheets
6	Measuring Tape

Resistivity and Gravity data acquisition and processing methods

Several steps were considered while acquiring data using the Resistivity method. After locating the suitable study area, the equipment was set up with a measured survey length of 200 meters. The resistivity cable was laid out at the length of 200 m with 100 m on each side of the Terrameter, selector, and battery which were placed at the centre of the survey line. Forty (40) electrodes were planted into the ground using a hammer with each electrode separated by a 5 m distance across the survey line. Following the placement of electrodes, jumpers were used to connect the electrodes with the takeout at the ABEM Lund Multi-Electrode Cable Connector. At the centre of the survey line, the Terrameter was connected to the 12 V sealed acid battery and also, and the Terrameter was then connected to the ABEM electrode selector ES 10- 64C using the connection cable. After the data acquisition phase was finished, the recorded data from the Terramater was transferred into the computer using the SAS4000, processed with the RES2DINV software to create a resistivity surface layer model, and then imported into ArcGIS software for additional analysis.

Likewise, many procedures were taken into account when gathering data through the Gravity approach. The initial step was to choose the ideal site for the base station. The tripod was then firmly placed on the flat surface after making sure the bubble on the tripod was plumbed at the centre. The Scrintex Microgravity Meter was carefully positioned on the tripod. Then, certain parameters such as the date, time, and the number of readings taken were set up on the microgravity meter by turning the knob on the machine. The survey was carried out based on a loop pattern, so, the base reading was obtained at every 3 hours interval. This step allows the loop pattern to be closed, followed by the opening of a new one. The reading with the lowest standard deviation is prioritized. The raw data from Scintrex Gravity Meter were exported into the computer and processed using Microsoft Excel. A few lists of errors and corrections such as free-air correction, Bouguer correction, and latitude correction were identified and corrected to produce Bouguer Anomaly. The processed and corrected data with parameters such as altitude, longitude, and Bouguer Anomaly were transferred to the ArcGIS software based on the surface gravity value using the WGS1984 file to create a contour map for further interpretation and analysis.

Results and Discussion

This section presents the findings and explanations of the resistivity and gravity methods used in the geophysical study. RES2DINV is the program needed to process the data in the resistivity survey, while ArcGIS is utilized to create a contour map based on the Bouguer anomaly that is computed from the gravity data points. The data is analysed to identify and pinpoint any potential karstic voids in the subsurface layers.

Figure 3: The map of the study area showing the location of the resistivity lines and gravity points (Google Earth, 2015).

Resistivity data interpretation

The RES2DINV application is used to analyze the pseudosection of the resistivity model to interpret the resistivity data. Based on the observed differences in resistivity values at various depths, this resistivity model characterizes the underlying layers and provides indications of the existence of abnormalities (such as karstic voids). In general, as the depth of the subsurface layers increases, so does the resistivity value. Six (6) different survey lines with a length of 200 meters for each line were conducted. The resistivity line has a penetration depth of up to 43 meters. To find the potential anomalies, the resistivity variations in each survey line were computed and then further analysed. Figures (4-9) display the resistivity pseudosection layers. The pseudosection of the resistivity profile along line 1, which runs from northwest to southeast, is displayed in Figure 4. Three distinct layers, each with a corresponding depth, make up the profile. The first layer has the lowest resistivity values between 0 and 190 Ωm and a depth of 0 to 7.45 meters. The low resistivity value may be attributed to the presence of the moist content on the surface of the profile. At depths between 7.45 and 14.0 meters, the resistivity value increases significantly, ranging from 190 to 750 Ωm. The zone where soil transitions to bedrock may be connected to the rise in resistivity levels. With depth values ranging from 14.0 to 43.0 meters, the resistivity values also range between 750 and 3500 Ωm, respectively. There is an irregularity in this stratum that could be interpreted as a region of voids filled with air. Because air has a nearly infinite resistivity, anomalies like air-filled empty areas and caves typically exhibit higher resistivity values than the underlying bedrock (Ismail and Anderson, 2012).

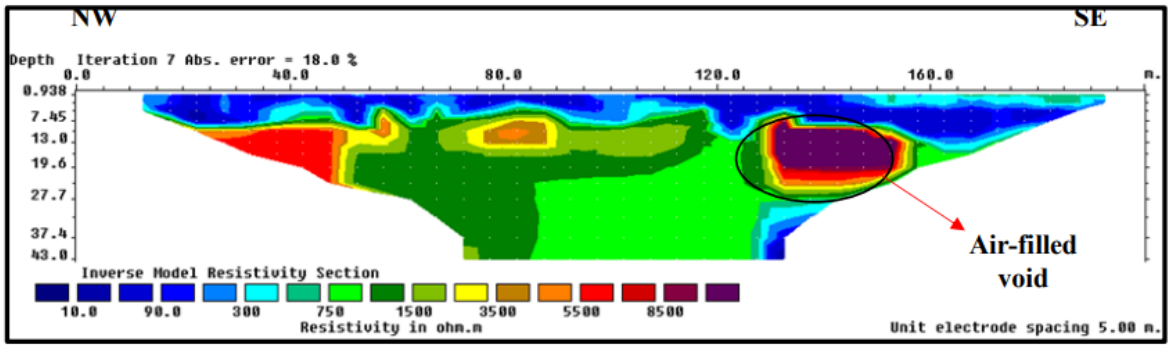

Figure 4: 2D Pseudo section for Resistivity Line 1

The processed pseudosection from survey line 2 is shown in Figure 5. Due to the differences in resistivity values, three distinct profile layers were observed, just like in Survey 1. The resistivity values at the topmost layer range from 0 to 300 Ωm, with their respective depth values ranging from 0 to 13.0 meters. The topsoil's exposure to weathering and propensity to contain loamy soil is thought to be the cause of the low resistivity reading at the first layer. In the layer, the resistivity values ranged from 300 to 950 Ωm at depths of 13.0 to 19.6 meters, respectively. The depth of the lowest layer ranges from 19.6 meters and above with the resistivity values ranging from 950 to 1500 Ωm where a couple of anomalies were observed. The resistivity value of these anomalies is higher than those of the nearby rock layers. The recorded resistivity of 10,000 Ωm indicates that this anomaly is represented by an air-filled cavity placed on a limestone environment of 5000 Ωm.

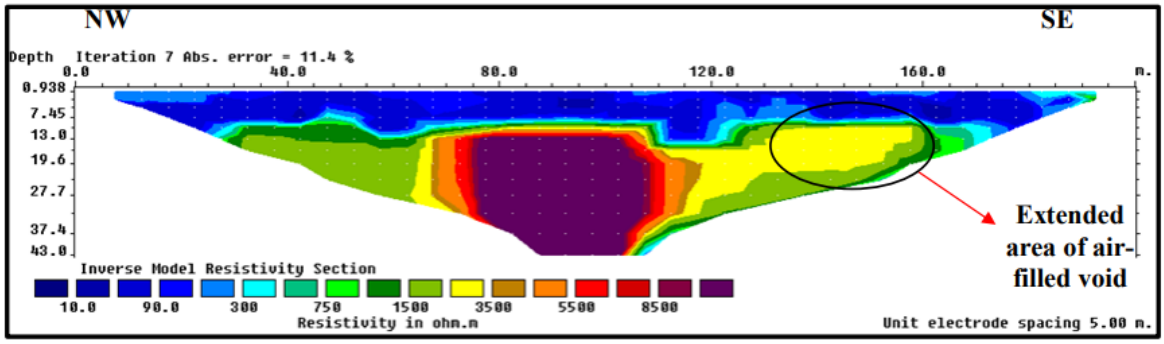

Figure 5: 2D Pseudosection for Resistivity Line 2.

The pseudosection of the resistivity profile taken at survey line 3 is displayed in Figure 6. The uppermost layer's depth values range from 0 to 13 meters, and their corresponding resistivity values are 0 and 190 Ωm. The top portion of the subsurface layer containing loamy soil may cause a low resistivity value. With resistivity values ranging from 190 to 750 Ωm, the middle section's depth values range from 13.0 to 15.0 meters, indicating a transition zone between the topsoil and the bedrock. The lowest portion of the pseudosection has a depth value from 15.0 to 43.0 meters, while the maximum resistivity values range between 750 and 3000 Ωm. A little air-filled vacuum could be the cause of the observed anomaly.

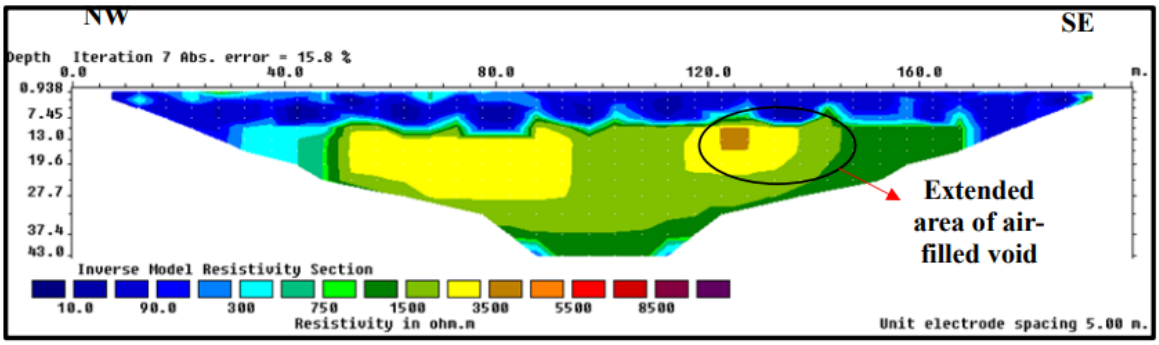

Figure 6: Resistivity pseudosection of survey line 3

The resistivity profile pseudosection at survey line 4 with characteristic depth values is displayed in Figure 7. The upper portion of the profile, whose depth values range from 0 to 13.0 meters, contains the layer with the lowest resistivity rating (0-190 Ωm). A low resistivity value typically denotes the existence of surfaces that are damp and rich in loam. The profile's middle layer is understood to be a transitional area that divides the bedrock from the loam-rich surface. This layer has resistivity values between 190 and 750 Ωm, with depth values of 13.0 and 19.6 meters, respectively. The resistivity value in the third layer of this survey line falls between 750 and 8500 Ωm at depths ranging from 19.6 to 43.0 meters. The higher resistivity value than the two previous layers may be attributed to the limestone present as stated by that the resistivity value of limestone can reach 100,000 Ωm.

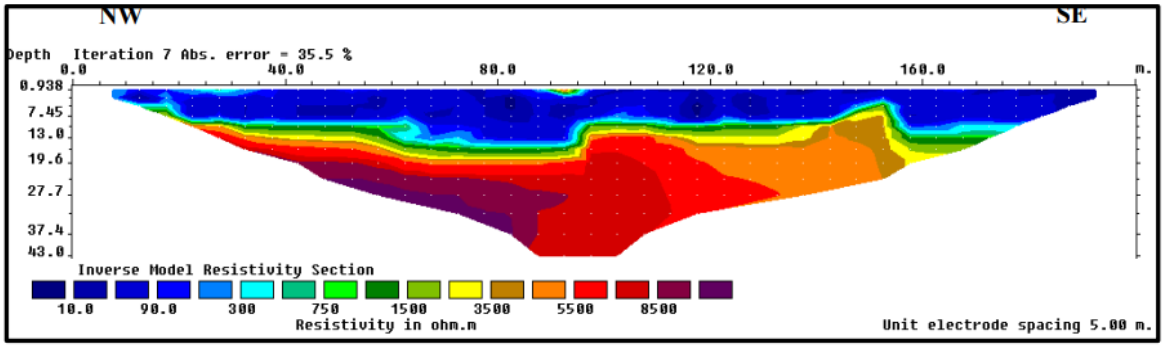

Figure 7: 2D Pseudosection for Resistivity Line 4

The survey line 5 pseudosection is shown in Figure 8. Three layers make up the profile, and each has been covered in further detail. With depth values ranging from 0 to 13.0 meters, the highest section of the profile has a reported resistivity value between 0 and 190 Ωm. The second layer is considered a transition zone with depth values between 13 and 19.6 meters and corresponding resistivity values between 300 and 1500 Ωm. The maximum resistivity value, which ranges from 3500 to 10,000 Ωm, is measured from 37.4 to 43.0 meters, respectively at the last layer. The existence of limestone formation is indicated by an increase in the resistivity value.

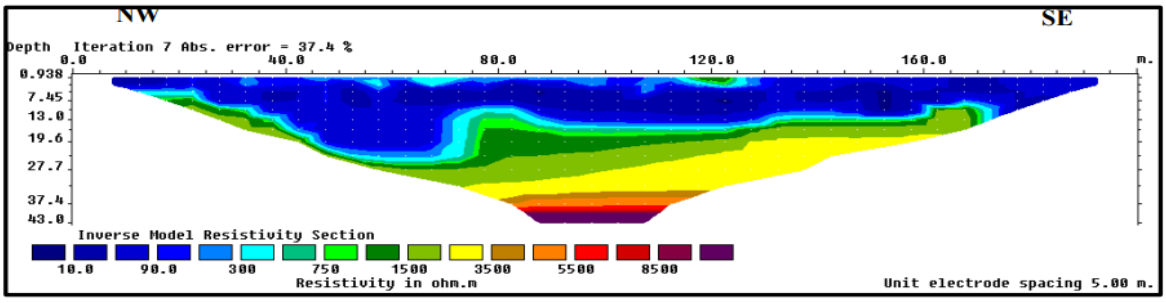

Figure 8: 2D Pseudosection for Resistivity Line 5

The resistivity profile pseudosection based on survey line 6 is displayed in Figure 9. The profile's uppermost portion displays the lowest resistivity values, which range from 0 to 300 Ωm. Because the top layer is primarily composed of clay or damp soil, the resistivity value is low. The resistivity values between 300 and 1500 Ωm were recorded at a depth of around 10.0 to 13.0 meters. This layer divides the bedrock from the topsoil. The resistivity profile's lowest layer shows the highest resistivity value, which is estimated to be around 1500 Ωm at a depth of roughly 13.0 to 43.0 meters. An area of worn bedrock and limestone is thought to be the source of the high resistivity layer.

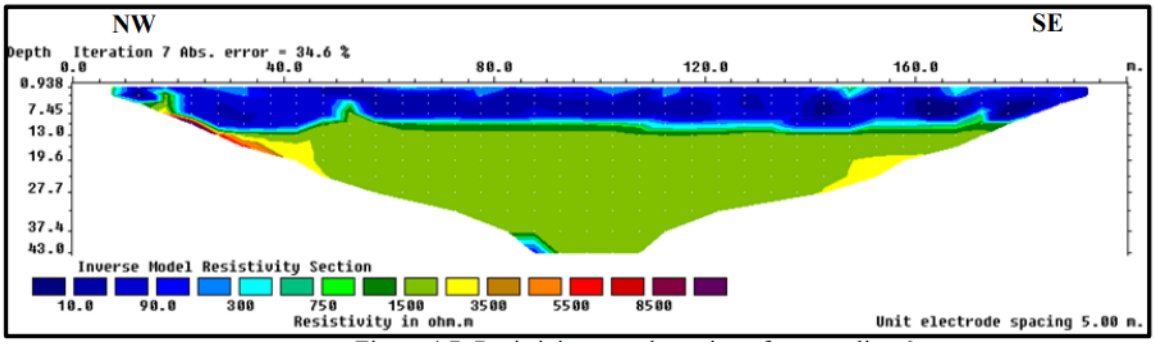

Figure 9: 2D Pseudosection for Resistivity Line 6

The pseudosection of the resistivity profile depicts the change of resistivity values at various depths of the subsurface layers based on the survey lines from Figures 4 to 9. The pseudosection is divided into three distinct layers at varying depths by the variations in resistivity values. A mixture of soil, clay, sand, and silt is associated with the lowest resistivity zone, which is represented by the upper layer. The second layer represents the transition zone between the bedrock and the loam-rich topsoil. The lowest subsurface layer exhibits the highest resistivity value, which is associated with the presence of limestone, which causes karstic voids to occur. A few anomalies to exist on several survey lines based on the resistivity profile results. The third layer of the resistivity profile serves as the primary foundation for these deviations.

Gravity data interpretation

The research region, situated at the palm oil plantation in Gua Musang, Kelantan, is seen on the Bouguer anomaly contour map in Figure 10. The range of the local gravity values is 5041.35 to 5830.07 mGal. The northeast region has the lowest value, 5041.35 mGal. However, low gravity values are also present in some parts of the southwest. The density of the underlying layers mostly determines the significance of the measured gravity result. The low-density area is thought to be an unconsolidated soil material that is most impacted by the puddles that form on the ground as a result of heavy rain. In the meantime, the yellow to gold range denotes the medium to high-density area. It is believed that there is an anomaly between resistivity survey lines 1 and 2 with a lower density value than the surrounding area. The reduced density of the anomaly is believed to be due to the possible presence of an air-filled gap in that area. The data from the resistivity survey conducted in this area is used to assist in interpreting the gravity study's findings. Survey lines 1 through 6 from the previous dipole-dipole survey are linked to the gravity survey to provide a more accurate understanding of the underlying layers. Finding any possible karstic voids is therefore easy and precise.

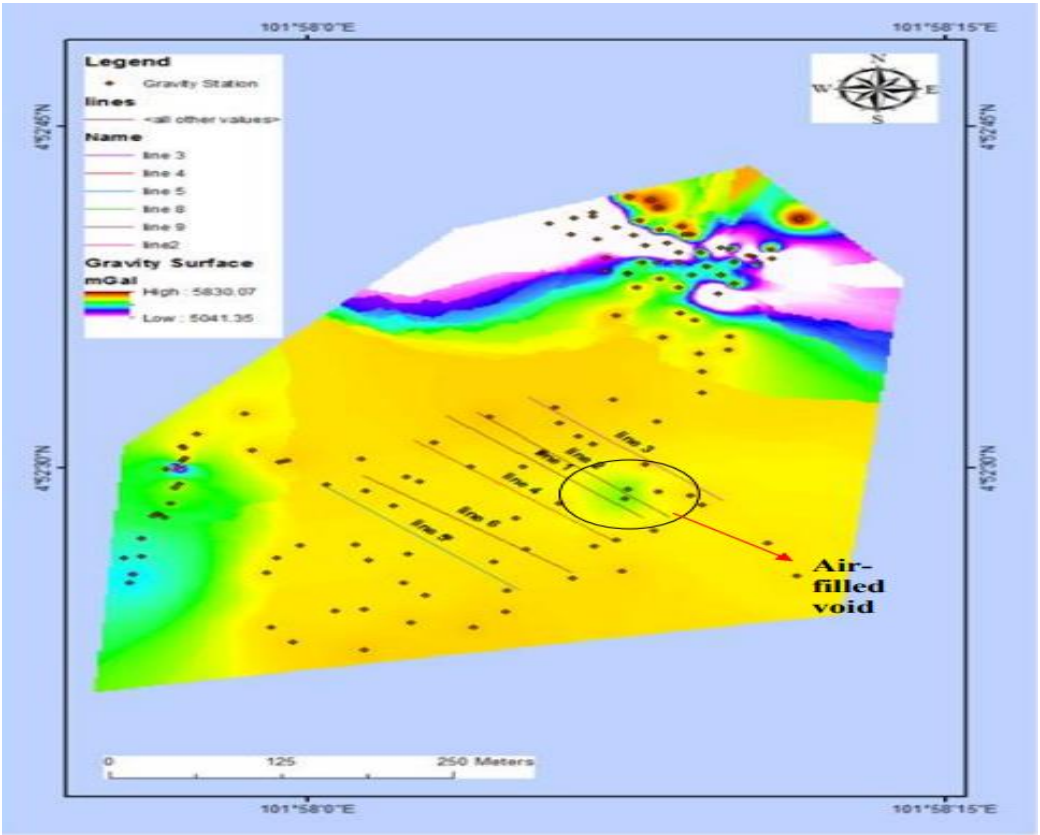

Figure 10: Bouguer anomaly map of the study area

Resistivity profile pseudosections were produced based on the 6 survey lines that range from northwest to southeast direction across the study area. The collected resistivity data were processed via RES2DINV programme to be further interpreted. Meanwhile, for gravity survey method, there are about 85 gravity points collected throughout the study area. This method involved the production of a Bouguer anomaly contour map by using ArcGIS software. Whereby, the values of Bouguer anomaly determine the anomalies present in the area, and assumptions are made. Based on pseudosection profiles and Bouguer anomaly of both resistivity and gravity survey respectively, a correlation is made between the two methods. A final interpretation is made to the generated contour map for the possible location of karstic void.

Conclusion

According to this study, karstic structures in the subsurface can be found and identified using geophysical (resistivity and gravity) methods. In the gravity method, the measured data are gravitational field of the Earth in space and time while its estimated property is density. Similarly, in Geo-electric method, the measured data is earth resistance and its estimated property is electrical resistivity. These methods are quite helpful and generally very user-friendly because of their features and specifications that are easy to use without requiring human participation. The specific location of these voids was further analysed using the Geographical Information System (GIS) to identify and map the subsurface karstic feature of Gua Musang. The data interpreted from the gravity method generated based on the Bouguer anomaly values were correlated with the interpretations of six resistivity survey lines. A clear picture of the subsurface, including variations in karstic structures and their fill or void status, was given by the contrast in Bouguer anomaly within the research area.

The observed anomaly is interpreted as a karstic void due to the variation in resistivity value between the anomaly and the surrounding rock. Based on the standard resistivity values range, the calculated resistivity value ranges between 50 to 400 Ωm. According to (Loke, 2011; Wilkinson *et al*., 2014a), this range of resistivity value is indicated by limestone layers which tend to form karst as a result of soil dissolution. Consequently, a significant likelihood of karstic features is indicated by the anomaly that affects the result. The combined methods gave a more accurate representation of the Earth's subsurface layers which in turn reduces uncertainty in void localization. Similar results were obtained as compared to the previous survey carried out in Gua Musang (Elhaj, 2016).

References

Ahmad, F., Yahaya, A. S., and Farooqi, M. A. (2006). Characterization and Geotechnical Properties of Penang Residual Soils with Emphasis on Landslides. *American Journal of Environmental Sciences*, 2(4): 121–128. https://doi.org/10.3844/ajessp.2006.121.128

Amaral, G., Bushee, J., Cordani, U. G., Kawashita, K., Reynolds, J. H., Almeida, F. F. M. D. E., de Almeida, F. F. M., Hasui, Y., de Brito Neves, B. B., Fuck, R. A., Oldenzaal, Z., Guida, A., Tchalenko, J. S., Peacock, D. C. P., Sanderson, D. J., Rotevatn, A., Nixon, C. W., Rotevatn, A., Sanderson, D. J., Junho, M. do C. B. (2013). Change detection of urban body. *Journal of Petrology*, 369(1): 1689–1699. https://doi.org/10.1017/CBO9781107415324.004

Bakhshipour, Z., Huat, B. B. K., Ibrahim, S., Asadi, A. and Kura, N. U. (2013). Application of geophysical techniques for 3D geohazard mapping to delineate cavities and potential sinkholes in the northern part of Kuala Lumpur, Malaysia. *The Scientific World Journal*, 2013: Article ID 629476, 11 pages. https://doi.org/10.1155/2013/629476

Chalikakis, K., Plagnes, V., Guerin, R., Valois, R. and Bosch, F. P. (2011). Contribution of geophysical methods to karst-system exploration: An overview. *Hydrogeology Journal*, 19(6): 1169–

1180. https://doi.org/10.1007/s10040-011-0746-x

Elhaj, K. G. E. M. K. (2016). Subsurface Delineation and Cavity Investigation Using Geophysical Methods in Gua Musang, Kelantan, Malaysia. *August*, 1–85. https://doi.org/10.13140/RG.2.2.33212.85129

Gambetta, M., Armadillo, E., Carmisciano, C., Stefanelli, P., Cocchi, L. and Tontini, F. C. (2011). Determining geophysical properties of a near-surface cave through integrated microgravity vertical gradient and electrical resistivity tomography measurements. *Journal of Cave and Karst Studies*, 73(1): 11–15. https://doi.org/10.4311/jcks2009ex0091

Gochenour, J. A., Suranovic, B. S., Gosselin, G. and Mcgary, R. S. (2017). Characterizing subsurface void spaces and water distribution and flow patterns in cave hill karst using resistivity. Senior Honors Projects, 2010-current. 266 https://doi.org/10.1130/abs/2017am-304674

Gochenour, J., McGary, R., Gosselin, G. and Suranovic, B. (2018). Investigating Subsurface Void Spaces and Groundwater in Cave Hill Karst Using Resistivity. 15th Sinkhole Conference Nckri Symposium 7. https://doi.org/10.5038/9780991000982.1041

Iqbal, M. F., and Khan, I. A. (2014). Spatiotemporal Land Use Land Cover change analysis and erosion risk mapping of Azad Jammu and Kashmir, Pakistan. *Egyptian Journal of Remote Sensing and Space Science*, 17(2): 209–229. https://doi.org/10.1016/j.ejrs.2014.09.004

Khoo, H. P. (1983). Mesozoic Stratigraphy in Peninsular Malaysia. *Workshop on Stratigraphic Correlation of Thailand and Malaysia*, 370–383.

Loke, M. H. (2011). Instrumentation, Electrical Resistivity. *Encyclopedia of Solid Earth Geophysics*. *January 2011*. https://doi.org/10.1007/978-90-481-8702-7

McGrath, R. J., Styles, P., Thomas, E. and Neale, S. (2002). Integrated high-resolution geophysical investigations as potential tools for water resource investigations in karst terrain. *Environmental Geology*, 42(5): 552–557. https://doi.org/10.1007/s00254-001-0519-2

Styles, P., McGrath, R., Thomas, E. and Cassidy, N. J. (2005). The use of microgravity for cavity characterization in karstic terrains. *Quarterly Journal of Engineering Geology and Hydrogeology*, 38(2): 155–169. https://doi.org/10.1144/1470-9236/04-035

Thode, H. G., Shima, M., Rees, C. E. and Krishnamurty, K. V. (1965). Erratum: Carbon-13 Isotope Effects in Systems Containing Carbon Dioxide, Bicarbonate, Carbonate, and Metal Ions. *Canadian Journal of Chemistry*, 43(8): 2451–2451. https://doi.org/10.1139/v65-336

Wilkinson, P. B., Uhlemann, S., Chambers, J. E., Meldrum, P. I. and Loke, M. H. (2014). Development and testing of displacement inversion to track electrode movements on 3-D electrical resistivity tomography monitoring grids. *Geophysical Journal International*, 200(3): 1566–1581. https://doi.org/10.1093/gji/ggu483

Zhou, W., Beck, B. F. and Adams, A. L. (2002). Effective electrode array in mapping karst hazards in electrical resistivity tomography. *Environmental Geology*, 42(8): 922–928. https://doi.org/10.1007/s00254-002-0594-z